A STUDY OF THE SENSITIZER IN THE LUMINESCENT SYSTEMS $(Y,Gd)_2O_2SO_4$:Bi,Tb AND $Li_6(Y,Gd)(BO_3)_3$:S,Tb (S= Ce^{3+},Pr^{3+} or Bi^{3+})

H.S. KILIAAN and G. BLASSE

Physical Laboratory, State University Utrecht, P.O. Box 80.000,
3508 TA Utrecht (The Netherlands)

Received 25 March 1987; accepted 21 April 1987

ABSTRACT

The luminescence of the systems $(Y,Gd)_2O_2SO_4$:Bi,Tb and $Li_6(Y,Gd)(BO_3)_3$:S,Tb (S= Ce^{3+},Pr^{3+} or Bi^{3+}) is reported, and the role of the sensitizer for the Gd^{3+} sublattice has been studied. Upon excitation into the sensitizers Bi^{3+} or Pr^{3+}, in both systems the excitation energy migrates from the sensitizer over the Gd^{3+} sublattice to the Tb^{3+} traps. We observed two different Bi^{3+} emissions at room temperature in the oxysulphate system, and at T < 120 K in the borate system. This is related to the formation of Bi^{3+} clusters which act as traps. The Ce^{3+} ion in the borate system functions as a trap. This is discussed and compared to other rare-earth-borate compounds, which leads to recommendations for the use of the Ce^{3+} ion as a sensitizer of the Gd^{3+} ion in RE-borate compounds.

INTRODUCTION

At the moment, much attention is paid to the luminescence of Gd^{3+} compounds (see e.g. [1–3]). From a fundamental as well as from a practical point of view, Gd^{3+} compounds have attractive properties.

In Gd^{3+} compounds the Gd^{3+} excitation energy migrates rapidly over the Gd^{3+} sublattice. In rare-earth (RE) activated Gd^{3+} compounds, this excitation energy can be completely transferred from Gd^{3+} to the activator, resulting in the characteristic activator emission. For efficient excitation the Gd^{3+} ion needs a sensitizer, since the $4f^7$ transitions on the Gd^{3+} ion have a very low absorption strength. A luminescent material with high efficiency may result if a suitable sensitizer is used.

In this paper we present a study of the luminescent properties of the following systems: (i) $(Y,Gd)_2O_2SO_4$:Bi,Tb (both 1 at.%) and (ii) $Li_6(Y,Gd)(BO_3)_3$:S,Tb (where S = Ce^{3+}, Pr^{3+} or Bi^{3+}; both S and Tb^{3+} are 1 at.%). The focus in case of the borates is mainly directed upon the Bi^{3+}-sensitized compounds.

0254-0584/87/$3.50

The luminescence of Bi^{3+} in $RE_2O_2SO_4$ has been investigated by Blasse and Bril [4]. From their data the Bi^{3+} is expected to sensitize the Gd^{3+} emission efficiently, since the spectral overlap is considerable.

For the $Li_6RE(BO_3)_3$ lattice such data are not available in the literature. We, therefore, tried to sensitize the Gd^{3+} emission with Ce^{3+}, Pr^{3+} or Bi^{3+}.

The crystal structure of both compounds is known. In the oxysulphate structure layers of composition RE_2O_2 can be distinguished [5]. The Gd^{3+}-Gd^{3+} distance within a layer is about 3.6 Å, and between successive layers about 4.3 Å. In the borate compound the RE^{3+} ions form linear zig-zag chains along the c-axis [6]. The shortest Gd^{3+}-Gd^{3+} distance in the chain, the intrachain distance, is about 3.9 Å and the Gd^{3+}-Gd^{3+} interchain distance is about 6.7 Å [7]. This compound has a one-dimensional RE^{3+} sublattice. The energy migration over the Gd^{3+} lattice in $Li_6Gd(BO_3)_3$ was studied before by Garapon et al. [7].

EXPERIMENTAL

The preparation of the bismuth- and terbium-doped rare-earth oxysulphate powder samples was carried out as described in [8] (see also Table I). The starting materials were Y_2O_3, Gd_2O_3, Tb_4O_7 (all from Highways Int.; 99.999%) and Bi_2O_3 (J.T. Baker; Baker Analyzed Reagent). Before firing, the obtained rare-earth hydrated sulphate was mixed with 3 grams $(NH_4)_2SO_4$ (Merck; p.a.).

Table I. Firing conditions for samples $RE_2O_2SO_4$: Bi^{3+}, Tb^{3+} and $Li_6RE(BO_3)_3$:S,Tb^{3+} (RE = Y^{3+}, Gd^{3+} and S = Ce^{3+}, Pr^{3+} or Bi^{3+}).

Sample	Firing temperature/°C	time/h	atmosphere
$RE_2O_2SO_4$	900 - 950	9-10	air
$Li_6RE(BO_3)_3$	730 - 770	24	N_2

The synthesis of the $Li_6RE(BO_3)_3$ powders, doped with bismuth, cerium or praseodymium and terbium was performed in a similar way as described in [9]. The oxides mentioned above were used, and further Li_2CO_3, H_3BO_3 (both from Merck; p.a.), CeO_2 (Highways Int.; 99.999%) and Pr_2O_3 (Fluka A.G.; 99.9%). The carbonate and oxides were mixed in a ball mill. The boric acid was added to this mix just before firing in a covered platinum crucible in a nitrogen atmosphere (see also Table I). All compounds were checked by X-ray powder diffraction.

The optical measurements were carried out at room temperature as described in [10].

RESULTS AND DISCUSSION

$(Y,Gd)_2O_2SO_4$:Bi,Tb

Samples of this composition show a Tb^{3+} emission of moderate intensity upon short-wavelength UV excitation. We measured a quantum efficiency of about 40% for $(Gd_{0.98}Bi_{0.01}Tb_{0.01})_2O_2SO_4$.

The excitation spectrum of the Tb^{3+} $^5D_4$ emission of $(Gd_{0.98}Bi_{0.01}Tb_{0.01})_2O_2SO_4$ is shown in Fig. 1. It consists of a broad band ($\lambda_{max} \approx 265$ nm) due to Bi^{3+} [4] and some lines ($\lambda_{max} \approx 275$, 280, 307 and 310 nm) due to Gd^{3+}. The longer wavelength part (not presented in Fig. 1) shows the characteristic Tb^{3+} lines.

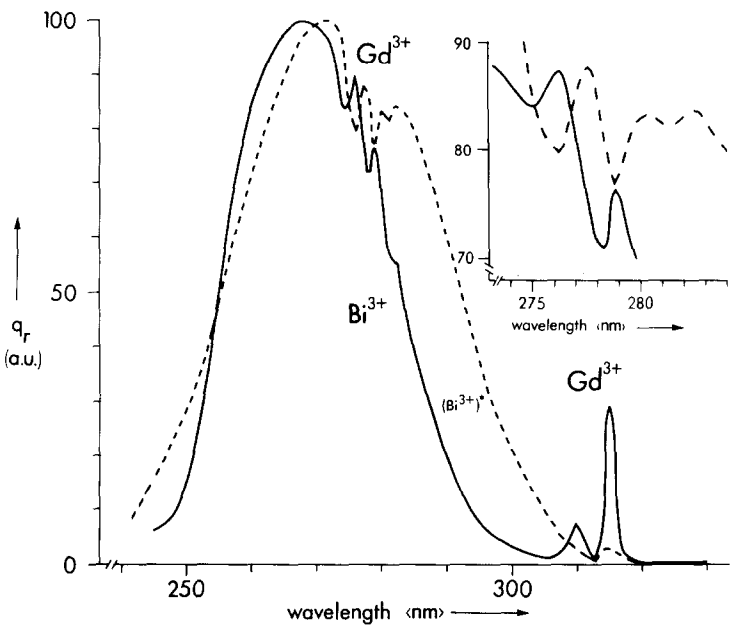

Fig. 1. Excitation spectra of the Tb^{3+} $^5D_4$ emission ($\lambda_{em} \approx 542$ nm) (solid curve) and the $(Bi^{3+})^*$ emission ($\lambda_{em} \approx 520$ nm) (broken curve) at room temperature for $(Gd_{0.98}Bi_{0.01}Tb_{0.01})_2O_2SO_4$ and $(Gd_{0.99}Bi_{0.01})_2O_2SO_4$, respectively; q_r gives the relative quantum output in arbitrary units.

Blasse and Bril [4] have ascribed the broad excitation band to the $^1S_0 \rightarrow {}^3P_1$ transition on the Bi^{3+} ion. The Gd^{3+} lines observed, are the $^8S_{7/2}$ to ^6P_J (round 310 nm) and to ^6I_J (round 275 nm) transitions.

Excitation into the Bi^{3+} ion yields an equal amount of Tb^{3+} $^5D_3$ and $^5D_4$ emission and a broad band (about 7% of the total emission intensity) with $\lambda_{max} \approx 520$ nm. For the time being this emission is indicated as $(Bi^{3+})^*$ emission.

We prepared a sample $(Gd_{0.99}Bi_{0.01})_2O_2SO_4$ to investigate the $(Bi^{3+})^*$ emission in more detail. Its excitation spectrum at RT is also plotted in Fig. 1. It is definitely different from the Tb^{3+} excitation spectrum mentioned above, although the differences are not large. There is a broad band ($\lambda_{max} \simeq 270$ nm) and a weak Gd^{3+} line at about 313 nm. The dips in the 270 nm band have their minima at 275, 278 and 280 nm. They coincide with the Gd^{3+} $^8S_{7/2} \rightarrow {}^6I_J$ transitions. They appear as dips, because at these wavelengths both $(Bi^{3+})^*$ and Gd^{3+} are excited, but most of the excited Gd^{3+} ions obviously do not transfer to $(Bi^{3+})^*$.

The $(Bi^{3+})^*$ emission is ascribed to clusters of Bi^{3+} ions. From the work on ns^2 ions, it is well known that single charged ns^2 ions can form clusters, e.g. pairs [11]. It has been shown that Bi^{3+} has the same tendency [12,13]. In their luminescence studies, Wolfert and Blasse [14] could not even observe isolated Bi^{3+} ions in LaOCl-Bi^{3+}, a compound which has also a RE_2O_2-layered structure [15]. In $Gd_2O_2SO_4$, these clusters act at 300 K as traps of the Gd^{3+} excitation energy, and partly even as killers, because the emission intensity of $(Bi^{3+})^*$ increases at lower temperatures. This explains the moderate value of the quantum efficiency mentioned above. The diffuse reflection spectrum shows a weak absorption band between 300 and 400 nm. Excitation into this band yields no luminescence, not even at 4.2 K. We ascribe this absorption band to more complex clusters of Bi^{3+} ions. The absorption band of the Bi^{3+} and the $(Bi^{3+})^*$ centres practically coincide (see Fig. 1).

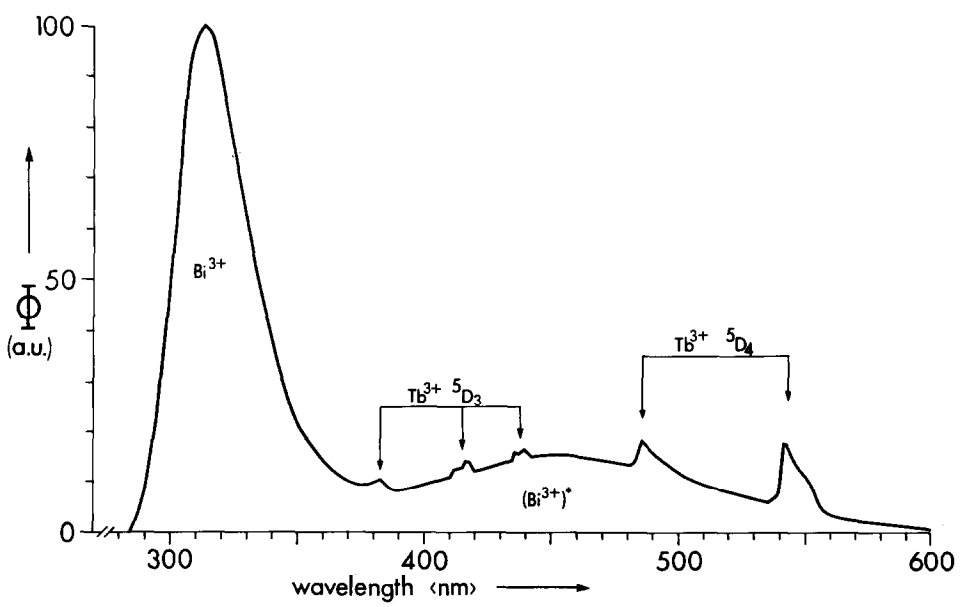

Fig. 2. Emission spectrum upon excitation into the Bi^{3+} ions ($\lambda_{exc} \simeq 265$ nm) room temperature for $(Y_{0.98}Bi_{0.01}Tb_{0.01})_2O_2SO_4$; Φ gives the spectral radiant power per constant wavelength interval in arbitrary units.

Figure 2 gives the emission spectrum of $(Y_{0.98}Bi_{0.01}Tb_{0.01})_2O_2SO_4$ for excitation into the Bi^{3+} ion. It consists of Bi^{3+} $^3P_1 \rightarrow {}^1S_o$ emission ($\lambda_{max} \approx 320$ nm) [4] and $(Bi^{3+})^*$ emission and some Tb^{3+} $^5D_3$ and $^5D_4$ emission.

From a comparison of the emission spectra for excitation into the Bi^{3+} ion of $(Gd_{0.98}Bi_{0.01}Tb_{0.01})_2O_2SO_4$ and of $(Y_{0.98}Bi_{0.01}Tb_{0.01})_2O_2SO_4$, the important role of the Gd^{3+} ions becomes clear. In the Gd^{3+} compound mainly Tb^{3+} emission is observed. In view of the low concentrations of Bi^{3+} and Tb^{3+} (both 1 at.%), the energy transfer from Bi^{3+} to Tb^{3+} takes place via the Gd^{3+} sublattice. This means that Bi^{3+} transfers its excitation energy to the Gd^{3+} ions (the Gd^{3+} $^8S_{7/2} \rightarrow {}^6P$ excitation lines and the Bi^{3+} emission band (Fig. 2) have an optimal spectral overlap), followed by migration over the Gd^{3+} sublattice to Tb^{3+}. In the yttrium compound the situation has changed drastically. Hardly any Tb^{3+} emission is observed, but a strong Bi^{3+} $^3P_1$-$^1S_0$ emission is observed (see Fig. 2). This illustrates the important role of the Gd^{3+} ions. We, therefore, have measured the integrated emission intensities as a function of the Gd^{3+} content at room temperature. The results are shown in Fig. 3. Note the strong increase of the Tb^{3+} emission intensity upon increasing Gd^{3+} content. The Bi^{3+} intensity drops rapidly upon introduction of Gd^{3+} into the yttrium lattice. The Gd^{3+} intensity shows a maximum.

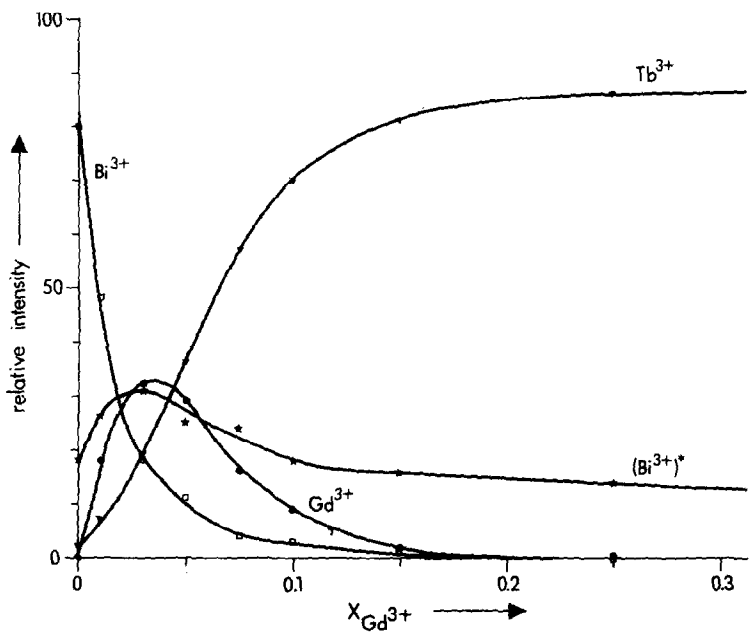

Fig. 3. The relative emission intensity of Bi^{3+} (□), Gd^{3+} (●), $(Bi^{3+})^*$ (x) and Tb^{3+} (▼) as a function of the Gd^{3+} concentration $x_{Gd^{3+}}$ at room temperature for $(Y_{0.98-x}Gd_xBi_{0.01}Tb_{0.01})_2O_2SO_4$. Excitation is into the Bi^{3+} ion.

The Bi^{3+} ion transfers its excitation energy to the Gd^{3+} ions. A critical distance for this transfer process, R_c, can be estimated from the decrease of the Bi^{3+} emission intensity shown in Fig. 3. This decrease of the Bi^{3+} emission as a function of the Gd^{3+} concentration, x, is given by:

$$I_{Bi^{3+}}(x) = I_{Bi^{3+}}(x=o).(1-x)^n \qquad (1),$$

where n is the number of Gd^{3+} neighbour sites to which Bi^{3+} can transfer its energy, and (1-x) gives the probability that such a site is not occupied by a Gd^{3+} ion. This implies that $Bi^{3+} \rightarrow Gd^{3+}$ transfer occurs if the Bi^{3+} ion has one or more Gd^{3+} neighbours, i.e. the n sites are within a sphere with radius R_c around the Bi^{3+} ion. Fitting the Bi^{3+} intensity curve (Fig. 3) to eqn. (1), gives $n \approx 25 \pm 5$. With this value and the crystal structure data of Table II, an estimate of R_c can be made: R_c has a value of about 7 Å. This means that Bi^{3+} in $Gd_2O_2SO_4$ is a very efficient sensitizer indeed.

Table II. Crystal structure data for $Gd_2O_2SO_4$ and $Li_6Gd(BO_3)_3$ and the calculated Gd-Gd distances.

Compound	lattice parameters	Gd-Gd distances in (Å)	number of neighbour ions	remark
$Gd_2O_2SO_4$	a = 4.18 Å b = 4.05 Å c = 12.98 Å $\alpha = \beta = \gamma = 90°$	3.63 4.05 4.18 4.3 5.8 5.9 6.0 6.8 6.9 7.1	4 2 2 1 4 2 2 4 4 8	
$Li_6Gd(BO_3)_3$	a = 7.23 Å b = 16.61 Å c = 6.66 Å $\beta = 105.32°$	3.88 6.65	2 2	intrachain interchain

It is also possible to calculate the value of R_c from the spectral overlap (SO) between the Gd^{3+} $^8S - {}^6P$ excitation lines and the Bi^{3+} emission band observed in Fig. 2. We considered electric dipole-dipole interaction, i.e.:

$$R_c^6 = 0.6 \times 10^{28}.(Q_{Gd^{3+}}).E^{-4}.SO \qquad (2)\ [16],$$

where the absorption cross-section of the Gd^{3+} ion ($Q_{Gd^{3+}}$) = 5 x 10^{-23} cm^2eV [17], E = 4 eV and the spectral overlap SO ≈ 2.6 eV^{-1}. We arrived at an R_c of about 4 Å. The difference between this value and the R_c value calculated above, indicates the important role played by exchange interaction in the transfer concerned. This has been observed before [18].

Let us now return to Fig. 3. Monitoring the Gd^{3+} emission as a function of the Gd^{3+} concentration ($x_{Gd^{3+}}$) makes it possible to estimate the critical concentration for energy migration (x_{cr}) among the Gd^{3+} ions as discussed in [3]. That paper considers the problem of percolation and critical concentration in a number of (Y,Gd)-systems. The theoretical value of x_{cr} is equal to $^2/N$, where N is the number of neighbour ions involved in the energy migration process [3].

The value of x_{cr} in the oxysulphate system is about 0.15. Therefore, N has a value of about 13. With this value for N and the crystal structure data presented in Table II, an estimate of R_{cr}, the critical distance for energy transfer among the Gd^{3+} ions, can be made: R_{cr} ≈ 6 Å. In this system energy transfer is by no means restricted to nearest neighbour ions. This implies that the Gd^{3+} energy migration is not restricted to the Gd_2O_2-layers. This value of R_{cr} is in line with the value of approximately 6.5 Å derived earlier for Gd^{3+} ions on a crystallographic site which lacks inversion symmetry. This is also the case in $Gd_2O_2SO_4$.

We measured for $Gd_2O_2SO_4$:Bi,Tb, upon excitation into the Bi^{3+} ion, an exponential Tb^{3+} $^5D_4$ decay curve with a decay time of about 2 msec. A single-exponential Gd^{3+} $^6P_{7/2} \rightarrow {}^8S_{7/2}$ decay curve with a decay time of 1 msec was measured for $(Gd_{0.5}Y_{0.48}Bi_{0.01}Tb_{0.01})_2O_2SO_4$. We have also tried to measure the $(Bi^{3+})^*$ decay in $(Gd_{0.99}Bi_{0.01})_2O_2SO_4$.

Figure 4 gives the decay curve at RT for excitation into the Bi^{3+} ions (λ_{exc} = 280 nm) with a one-exponential tail with a decay time of about 500 μsec. The build-up is not easy to analyze since all types of Bi^{3+} ions are excited simultaneously. However, it reflects feeding via the Gd^{3+} sublattice. The decay time of the tail is long compared to other Bi^{3+}-pair decay times, as measured by Wolfert et al. [12]. Obviously the decay time is not determined by the (fast) relaxation in the $(Bi^{3+})^*$ centre, but by the (relatively slow) feeding. This can be described following, e.g., the lines of argument for Cr^{3+} in MgO, given by Mac Craith et al. [19]. Apart from the build-up, the decay curve is expected to show a fast and a slow part. The fast part is due to direct excitation of $(Bi^{3+})^*$ followed by emission with a probability $P_{(Bi^{3+})^*}$. The intensity decreases as $I = I_o\exp[-P_{(Bi^{3+})^*}.t]$. For the slow part the time dependence is given by $\exp[-(P_{Gd} + P_{tr}).t]$, where P_{tr} is the overall Gd^{3+} to $(Bi^{3+})^*$ energy transfer probability, and P_{Gd} is the radiative probability of the Gd^{3+} ions. In our case we cannot measure the faster part. The slower part of the $(Bi^{3+})^*$ decay curve yields an acceptable value for $P_{Gd} + P_{tr}$, viz. 2 x $10^3 s^{-1}$ [30].

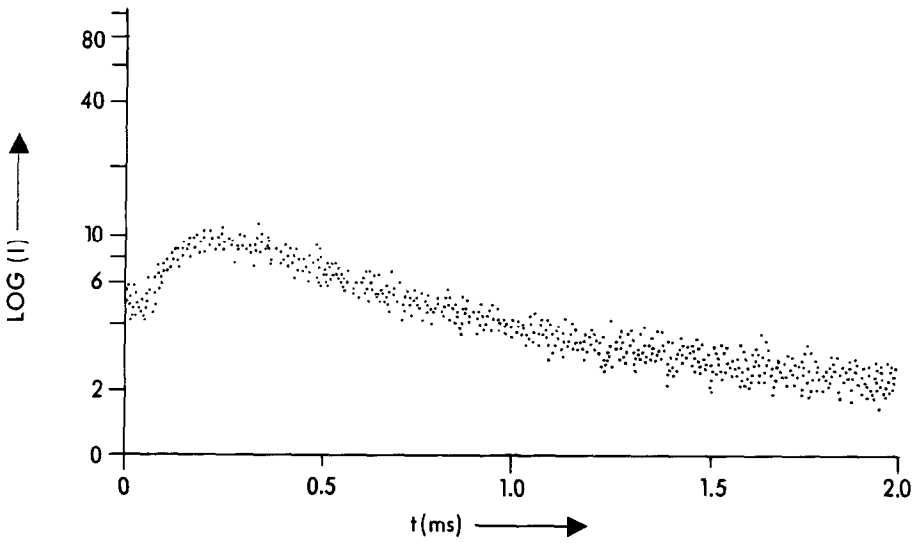

Fig. 4. The decay curve of the $(Bi^{3+})^*$ emission of $(Gd_{0.99}Bi_{0.01})_2O_2SO_4$ at room temperature. Excitation with $\lambda_{exc} \simeq 280$ nm (Bi^{3+}).

$\underline{Li_6(Y,Gd)(BO_3)_3:Bi,Tb}$

The samples of $Li_6(Y,Gd)(BO_3)_3$:Bi,Tb have a pale-yellow colour. This colour seems to be related to the presence of the Bi^{3+} ions, since the Ce^{3+}, Tb^{3+}- and Pr^{3+}, Tb^{3+}-doped samples (see below) are colourless. Therefore, we prepared the following samples: (i) $Li_6Gd_{0.98}Bi_{0.01}Tb_{0.01}(BO_3)_3$, (ii) $Li_6Gd_{0.985}Bi_{0.005}Tb_{0.01}(BO_3)_3$ and (iii) $Li_6Gd_{0.9875}Bi_{0.0025}Tb_{0.01}(BO_3)_3$. From (i) to (iii) the yellow colour becomes less intense, and the third sample is nearly colourless. For short wavelength UV excitation, there is an increase of the Tb^{3+} emission intensity and a decrease of the Bi^{3+} emission intensity going from sample (i) to (iii), while the Gd^{3+} emission intensity remains the same for all samples. Below we will show that the transfer processes in the borate system are the same as in the oxysulphate system. Therefore, this intensity change shows that the Bi^{3+} ion is not in a second phase: less Bi^{3+} results in more Tb^{3+} emission, suggesting that at least part of the Bi^{3+} ions are competing with the Tb^{3+} for the Gd^{3+} excitation energy (as in the oxysulphate system). Therefore we assign the yellow colour tentatively to Bi^{3+} clusters, as in the oxysulphate system. These clusters act as killers at room temperature. The diffuse reflection spectra show an absorption tail extending to 500 nm, which is responsible for the yellow colour. Upon decreasing the Bi^{3+} concentration, the killer concentration decreases also, and therefore, more Tb^{3+} emission is observed.

At temperatures below 120 K, a $(Bi^{3+})^*$ emission band with $\lambda_{max} \simeq 540$ nm appears in the emission spectrum of $Li_6Y_{0.98}Bi_{0.01}Tb_{0.01}(BO_3)_3$ upon excitation into the Bi^{3+} ion.

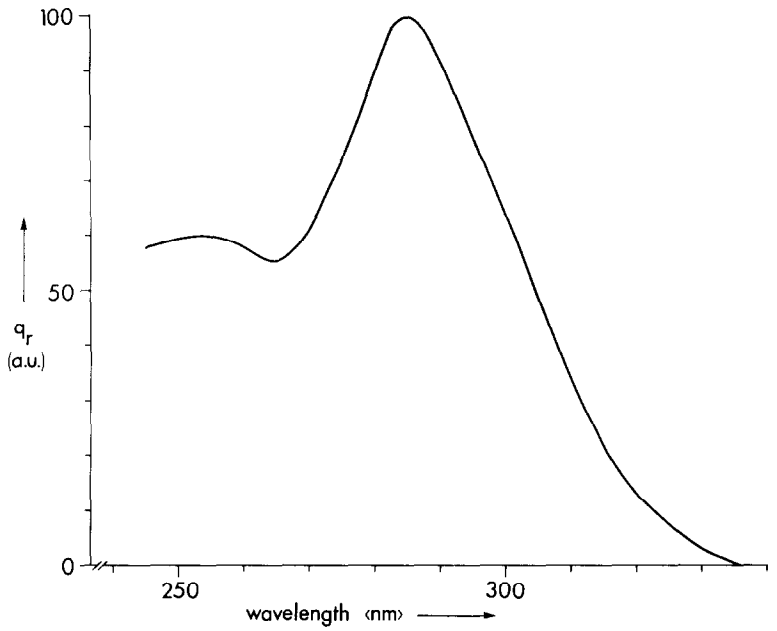

Fig. 5. Excitation spectrum of the $(Bi^{3+})^*$ emission (λ_{em} = 520 nm) at 4.2 K for $Li_6Y_{0.98}Bi_{0.01}Tb_{0.01}(BO_3)_3$.

Its excitation spectrum is shown in Fig. 5. This excitation region corresponds to the shorter-wavelength part of the absorption tail in the reflection spectra.

The quantum efficiency of the luminescence of $Li_6Gd(BO_3)_3$:Bi,Tb upon Bi^{3+} excitation has a low value (about 20%). The Bi^{3+} killers proposed above are responsible for the fact that it was not possible to obtain samples with high quantum efficiencies.

In Fig. 6 the excitation spectrum of the Tb^{3+} $^5D_4$ emission of $Li_6Gd_{0.98}Bi_{0.01}Tb_{0.01}(BO_3)_3$ is shown. A broad Bi^{3+} $^1S_0 \rightarrow {}^3P_1$ absorption band with λ_{max} = 265 nm, and the Gd^{3+} $^8S_{7/2}$ to ^6P lines are observed. The longer wavelength part with the characteristic Tb^{3+} lines is not presented.

Excitation into the Bi^{3+} band yields about 10% Bi^{3+} $^3P_1 \rightarrow {}^1S_0$ emission, 5% Gd^{3+} ^6P emission and about 85% Tb^{3+} $^5D_4$ emission. Due to multiphonon relaxation, no Tb^{3+} $^5D_3$ to ^7F_J emission is observed.

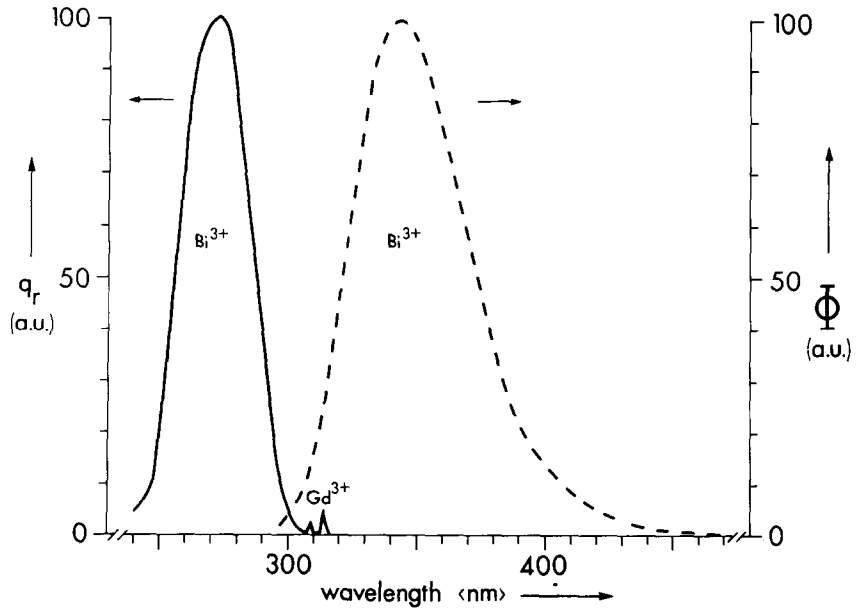

Fig. 6. Excitation spectrum of the Tb^{3+} $^5D_4$ emission (λ_{em} = 542 nm) for $Li_6Gd_{0.98}Bi_{0.01}Tb_{0.01}(BO_3)_3$ (solid curve) and the emission spectrum upon excitation into the Bi^{3+} ion for $Li_6Y_{0.98}Bi_{0.01}Tb_{0.01}(BO_3)_3$ (broken curve), both at room temperature.

The emission spectrum of $Li_6Y_{0.98}Bi_{0.01}Tb_{0.01}(BO_3)_3$ consists of a Bi^{3+} $^3P_1 \rightarrow {}^1S_0$ emission band ($\lambda_{max} \approx 340$ nm) if excitation is into the Bi^{3+} band at 265 nm (Fig. 6). From both the emission spectra of $Li_6Gd_{0.98}Bi_{0.01}Tb_{0.01}(BO_3)_3$ and $Li_6Y_{0.98}Bi_{0.01}Tb_{0.01}(BO_3)_3$ the important role of the Gd^{3+} ions is clear: the energy transfer from Bi^{3+} to Tb^{3+} takes place via the Gd^{3+} ions. We have measured the relative Gd^{3+}, Bi^{3+} and Tb^{3+} emission intensities as a function of the Gd^{3+} concentration (x_{Gd}). Results are given in Fig. 7. The Tb^{3+} emission intensity increases and the Bi^{3+} emission intensity decreases with increasing Gd^{3+} concentration. Up to $x_{Gd} = 0.98$ the Gd^{3+} emission is present. This means that the Gd^{3+} concentration does not reach the critical concentration x_{cr} as in the oxysulphates (above). The energy transfer probability from Bi^{3+} to Gd^{3+} can be calculated in the same way as above, applying eqn. (2), with $Q_{Gd^{3+}} = 5 \times 10^{-23}$ cm^{2}eV, E = 4 eV and S0 = 0.05 eV^{-1}. This results in an R_c value of about 3 Å. Since the shortest Bi^{3+}-Gd^{3+} distance is about 3.9 Å (see Table II), this excludes a dominating contribution to the $Bi^{3+} \rightarrow Gd^{3+}$ energy transfer by electric dipole-dipole interaction. Therefore this transfer must be dominated by exchange interaction, which makes it hard to calculate R_c.

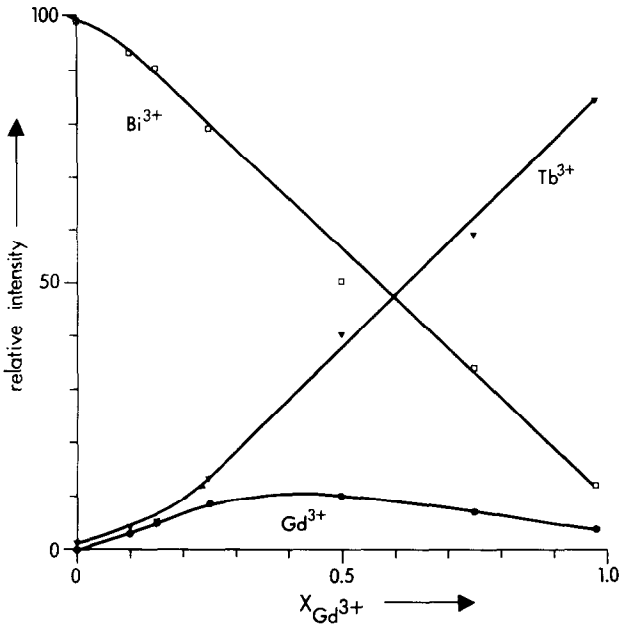

Fig. 7. The relative emission intensities of Bi^{3+} (□), Gd^{3+} (●) and Tb^{3+} (▼) as a function of the Gd^{3+} concentration $x_{Gd^{3+}}$ at room temperature for $Li_6Y_{0.98-x}Gd_xBi_{0.01}Tb_{0.01}(BO_3)_3$. Excitation is into the Bi^{3+} ion.

From the decrease of the Bi^{3+} emission intensity in Fig. 7, we can estimate a value for R_c. The value of n in eqn. (1) is found to be about 1. This value indicates that there is only one Gd^{3+} site within a sphere with radius R_c to which Bi^{3+} can transfer its excitation energy. In view of the structural data in Table II, R_c is 3.9 Å.

In $Li_6Gd(BO_3)_3$ the Bi^{3+} ion is not an efficient sensitizer. Not only does it not transfer its excitation energy completely to the Gd^{3+} ions, but its presence results also in killer centres.

$\underline{Li_6Gd(BO_3)_3:Ce,Tb}$

Samples $Li_6Gd(BO_3)_3$:Ce,Tb show only a very weak Tb^{3+} emission upon short wavelength UV excitation.

In Fig. 8 the luminescence spectra of $Li_6Gd_{0.98}Ce_{0.01}Tb_{0.01}(BO_3)_3$ are shown. The excitation spectrum of the Tb^{3+} $^5D_4$ emission shows at least three broad Ce^{3+} 4f → 5d bands at about 345 nm, 305 nm and below 250 nm. Further, the Gd^{3+} $^8S_{7/2}$ to ^6P, ^6I and ^6D transitions are clearly observed. Excitation into one of the Ce^{3+} bands yields mainly Ce^{3+} emission with $\lambda_{max} \simeq$ 415 nm, 385 nm and 325 nm.

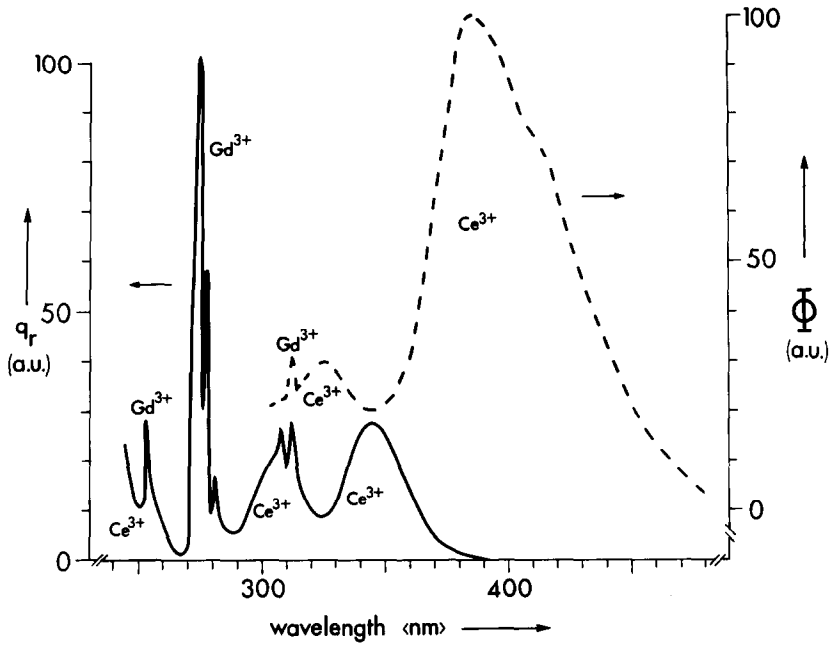

Fig. 8. Excitation spectrum of the Tb^{3+} $^5D_4$ emission ($\lambda_{em} \simeq 542$ nm) (solid curve) and the emission spectrum upon excitation with $\lambda_{exc} = 274$ nm (broken curve), both for $Li_6Gd_{0.98}Ce_{0.01}Tb_{0.01}(BO_3)_3$ at room temperature.

The energy difference of about 2000 cm^{-1} between the 385 nm and the shoulder at 415 nm corresponds to the ground state splitting $^2F_{7/2} - {}^2F_{5/2}$. Peculiarly enough, there is another Ce^{3+} emission band at shorter wavelength with a maximum at about 325 nm. Whereas the 415 and 385 nm-emission bands originates from the lowest crystal-field components (d_1) of the 5d state, the 325 nm-emission originates from the one-but lowest (d_2). In fact the excitation and emission spectra correspond nicely in this aspect. Similar phenomena have been observed before [20]. Obviously the rate of the non-radiative transition $d_2 \rightarrow d_1$ is not much larger than the d_2 radiative rate.

The energy transfer processes between Ce^{3+} and Gd^{3+} in $Li_6Gd(BO_3)_3$ become very complicated in this way. However, by neglecting transfer from a broad-band donor to a narrow-line acceptor relative to transfer from a narrow-line donor to a broad-band acceptor if the spectral overlap is of comparable size [21], we arrive at the following scheme: (i) excitation into the Ce^{3+} ion gives mainly Ce^{3+} emission, the transfer rate $Ce^{3+}(d_2) \rightarrow Gd^{3+}(^6P_{7/2})$ being negligibly small in comparison with the reverse transfer rate; (ii) excitation into the Gd^{3+} ion gives mainly Ce^{3+} and a small amount of Tb^{3+} emission. After excitation of the Gd^{3+} sublattice, the excitation energy migrates over the Gd^{3+} sublattice. The Ce^{3+} ion will be a much more effective trapping centre than the Tb^{3+} ion in view of the allowed transitions in the former [22]. As a consequence not much Tb^{3+} emission is observed.

Summarizing, the Ce^{3+} ion in $Li_6Gd(BO_3)_3$ behaves as an activator, not as a sensitizer. This is a surprising result, since in the borate $GdMgB_5O_{10}$ the Ce^{3+} ion behaves clearly as a sensitizer [2]. Both crystal structures have the rare-earth ions in an eight coordination forming linear zig-zag chains. In GdB_3O_6, the Ce^{3+} ion behaves also as a sensitizer, although a little less efficient than in $GdMgB_5O_{10}$ [13]. However, in $REAl_3B_4O_{12}$ and the orthoborates the Ce^{3+} absorption and emission levels are again too low for sensitization ([23] and [20], respectively), as is also the case for $SrLaBO_4$ [24]. It would be useful to have a rule of thumb to predict whether the Ce^{3+} ion in borates will be a sensitizer or an activator, because the borates are host-lattices of considerable importance.

The position of the Ce^{3+} levels of the 5d state is determined by two effects, *viz.* covalency, reducing the centre of gravity of the 5d state, and the symmetry and magnitude of the crystal-field at the Ce^{3+} site [20,25]. Cubic eight-coordination is unfavourable for a high position of the lower crystal-field components [20]. It seems, therefore, that covalency effects are more important [25]. If we consider for simplicity the borate group coordinating the Ce^{3+} ion as a polarizable medium, the strongest Ce-O covalency is expected for the borate group coordinated on the other side by low-charged ions. This simple model is unexpectedly succesful: in $GdMgB_5O_{10}$ and GdB_3O_6 these other-side ions are B^{3+} (and Mg^{2+}); in $GdAl_3B_4O_{12}$, $Li_6Gd(BO_3)_3$ and $GdBO_3$, they are trivalent ions larger than B^{3+} (and Li^+). The compound $SrLaBO_4$ is a case apart, since there is also an O^{2-} ion not belonging to a borate group, a situation which yields a high covalency anyhow. This predicts that only Gd^{3+} borates with condensed borate groups can be expected to show efficient sensitization with Ce^{3+}.

Finally we consider the Pr^{3+} ion as a sensitizer.

$Li_6Gd(BO_3)_3$:Pr,Tb

Upon excitation into the Pr^{3+} ion (λ_{exc} = 254 nm) $Li_6Gd_{0.98}Pr_{0.01}Tb_{0.01}(BO_3)_3$ yields mainly Tb^{3+} emission. No Pr^{3+} emission is observed. The Tb^{3+} excitation spectrum in Fig. 9 shows that Pr^{3+} is a sensitizer of the Gd^{3+} sublattice. There is energy transfer from Pr^{3+} to Gd^{3+}, followed by energy migration over the Gd^{3+} sublattice to the Tb^{3+} ions. Since the maximum of the Pr^{3+} excitation band is on or outside the spectral limit of our instrument, it is hard to indicate how efficient the transfer is. The absence of Pr^{3+} $4f5d \rightarrow 4f^2$ emission suggests that the transfer efficiency is high. A rough estimation of the energy difference between the positions of the lowest 4f-5d absorption bands of Pr^{3+} and Ce^{3+} yields about 13.000 cm^{-1}, in good agreement with expectation [28].

Efficient sensitization by Pr^{3+} has also been reported by De Hair for $BaGd_4Si_5O_{17}$ [26] and Srivastava *et al.* for $GdBO_3$ [27]. The criteria for this to occur have been given by De Vries and Blasse [28]. Actually these are satified in the present case. From the Ce^{3+}-doped compound the Stokes shift is seen to be relatively small. Figure 9 suggests that

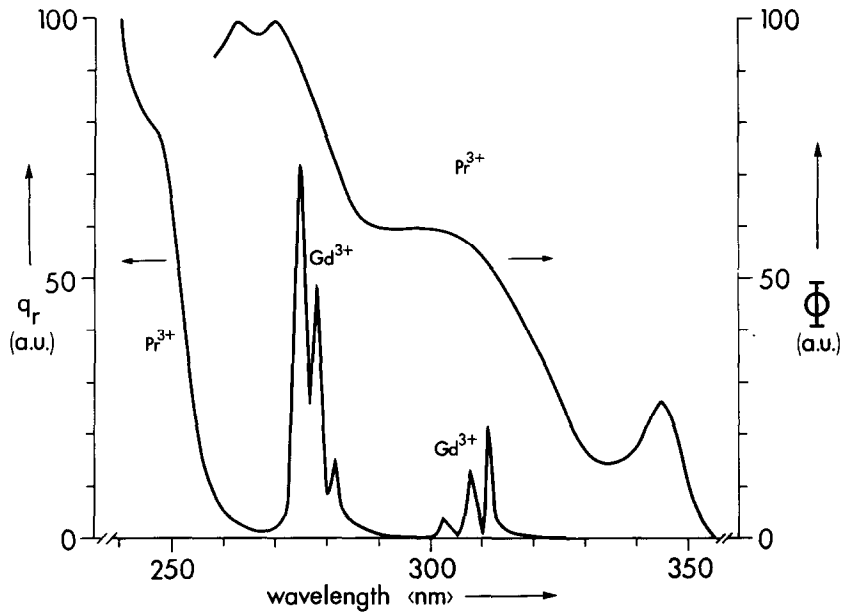

Fig. 9. Excitation spectrum of the Tb^{3+} $^5D_4$ emission ($\lambda_{em} \approx 542$ nm) for $Li_6Gd_{0.98}Pr_{0.01}Tb_{0.01}(BO_3)_3$ and the emission spectrum upon excitation with $\lambda_{exc} = 235$ nm of $Li_6Y_{0.99}Pr_{0.01}(BO_3)_3$, both at room temperature.

the Pr^{3+} $4f5d \rightarrow 4f^2$ emission will overlap the Gd^{3+} ^6I transitions. This is actually the case. The emission spectrum of $Li_6Y_{0.99}Pr_{0.01}(BO_3)_3$ shows two broad Pr^{3+} bands at about 270 nm and 300 nm and a weaker Pr^{3+} band at about 345 nm (Fig. 9). They are transitions from the lowest crystal-field component of the 4f5d state to the $^3H_4$ and $^3H_5$ levels, to the $^3H_6$ and ^3F_J levels, and to the $^1G_4$ level of the $4f^2$ configuration, respectively.

The Pr^{3+} ion is, therefore, the most efficient sensitizer in $Li_6Gd(BO_3)_3$. For practical applications it is situated at too high energy. Recently it has been shown that the use of Pr^{3+} yields also undesirable effects, viz. back-transfer from the activator to the sensitizer [29].

CONCLUSION

We have shown that Bi^{3+} and Pr^{3+} can sensitize the Gd^{3+} sublattice of $Li_6Gd(BO_3)_3$ and Bi^{3+} that of $Gd_2O_2SO_4$. However, these sensitizers have drawbacks resulting in radiationless losses. The Ce^{3+} ion in $Li_6Gd(BO_3)_3$ acts as an activator. Only in condensed borates, Ce^{3+} is expected to behave as a sensitizer.

ACKNOWLEDGEMENTS

The authors are indebted to Mr. R.J. Pet of the Philips Lighting Division, Eindhoven, The Netherlands, for his useful advice on the synthesis of the samples.

The investigations were supported by the Netherlands Foundation for Chemical Research (SON) with financial aid from the Netherlands Foundation for Technical Research (STW).

REFERENCES

1 J.Th.W. de Hair, J. Lumin., 18/19 (1979) 797.

2 J.Th.W. de Hair and J.T.C. van Kemenade, paper no. 54 presented at the Third International Symposium on the Science and Technology of Light Sources, Toulouse, 18-21 April 1983.

3 A.J. de Vries, H.S. Kiliaan and G. Blasse, J. Solid State Chem. 65 (1986) 190.

4 G. Blasse and A. Bril, Philips Res. Repts., 23 (1968) 461.

5 J.A. Fahey, in: C.E. Lundin, Proc. Rare Earth Res. Conf. 12th, (1976) 762.

6 G.K. Abdullaev, Kh.S. Mamedov, P.F. Rza-Zade, Sh.A. Guseinova and G.G. Dzhafarov, Russ. J. Inorg. Chem., 22 (1977) 1765.

7 C.T. Garapon, B. Jacquier, J.P. Chaminade and C. Fouassier, J. Lumin., 34 (1985) 211.

8 J.W. Haynes and J.J. Brown Jr., J. Electrochem. Soc., 115 (1969) 1060.

9 J. Mascetti, C. Fouassier and P. Hagenmuller, J. Solid State Chem., 50 (1983) 204.

10 A.C. van der Steen, J.J.A. van Hesteren and A.P. Slok, J. Electrochem. Soc., 128 (1981) 1327.

11 T. Tsuboi, Phys. Rev., B29, (1984) 1022.

12 A. Wolfert, E.W.J.L. Oomen and G. Blasse, J. Solid State Chem., 59 (1985) 280.

13 Hao Zhiran and G. Blasse, Mater. Chem. Phys., 12 (1985) 257.

14 A. Wolfert and G. Blasse, Mat. Res. Bull., 19 (1984) 67.

15 D.H. Templeton and C.H. Dauben, J. Amer. Chem. Soc., 75 (1953) 6069.

16 D.L. Dexter, J. Chem. Phys., 21 (1953) 836.

17 W.T. Carnall in K.A. Gschneidner Jr. and L. Eyring (eds.), Handbook on the Physics and Chemistry of Rare Earths, Vol. 3, North-Holland, Amsterdam, 1979, Chap. 24.

18 M. Leskelä, M. Saakes and G. Blasse, Mat. Res. Bull., 19 (1984) 151.

19 B.D. MacCraith, T.J. Glynn, G.F. Imbusch and C. McDonagh, J. Phys. C., 13 (1980) 4211.

20 G. Blasse and A. Bril, J. Chem. Phys., 47 (1967) 5139.

21 G. Blasse, Mater. Chem. Phys., 16 (1987) 201.

22 A.J. de Vries, W.J.J. Smeets and G. Blasse, Mater. Chem. Phys., submitted

23 F. Kellendonk, T. van der Belt and G. Blasse, J. Chem. Phys., 76 (1982) 1194.

24 Hao Zhiran and G. Blasse, J. Solid State Chem., 55 (1984) 23.

25 M.J.J. Lammers and G. Blasse, J. Electrochem. Soc., in press

26 J.Th.W. de Hair, J. Solid State Chem., 33 (1980) 33.

27 A.M. Srivastava, M.T. Sobieraj, S.K. Ruan and E. Banks, Mat. Res. Bull., 21 (1986) 1455.

28 A.J. de Vries and G. Blasse, Mat. Res. Bull., 21 (1986) 683.

29 A.J. de Vries, G. Blasse and R.J. Pet, to be published.

30 A.J. de Vries and G. Blasse, J. Physique, 46 (1985) C7-109.